Tc-2017-160

Response to RC1

Reviewer 1 (RC1), Received and published 13 September 2017.

Reviewer 1's general comments:

In this paper, the albedo and surface temperature of the glaciers in the Queen Elizabeth Islands (QEI) are investigated using MODIS data products for 2001 – 2016. Over the study period BSA is shown to decrease significantly in the month of July, while LST increases during the summer months (JJA). This is a valuable paper and it is well written (though a bit long) and technically sound. My comments below are almost all optional.

I believe that the authors have not fully taken advantage of this opportunity to explore the relationship between albedo and LST. Though they point out that albedo and LST are negatively correlated for the QEI, they do not discuss that relationship as cause-and-effect in either the Abstract or the Conclusion. The relationship between albedo and LST is discussed in Section 4.2 but I would have liked that discussion to have been better integrated throughout the paper. Since there was quite a bit of information about LST in the paper, the authors might want to consider including LST in the title of the manuscript.

The authors say that only the month of July shows statistically-significant albedo decrease over the study period. Thus, they should consider stating that the July albedo is decreasing over the study period instead of saying mean summer (JJA) albedo is decreasing.

If the paper can be made more concise it would be easier to follow.

Author's response to R1 general comment:

We thank the reviewer for the thoughtful evaluation of our manuscript. We have reviewed and addressed both the major considerations and minor specific comments.

1. **RC** refers to reviewer's comment
2. **AR** refers to author's response
3. Revised sections of the manuscript are presented in *italics*.

RC: If the paper can be made more concise it would be easier to follow.

AR: The paper has been revised to make it more concise and easier to follow. Sections 3.3 (now section 3.4) and 4.1 (now section 4) have been shortened. Repetition in sections 3.3 and 4.1 has been removed. Sections 4.1 and 4.2 have been merged (now section 4).

Revised text:

Revised Section 3.4, Lines 365-392:

> *'**3.4 Principal Components Analysis***
>
> *To explore whether there are any other spatial patterns in the 16-year mean summer BSA record that differ from the long-term (linear) trend, we performed a Principal Components Analysis of the BSA record (Sect. 2.3). The first and second Principal Components (Fig. 8) explain 65% and 12% of the variance in the mean summer BSA record, respectively. The spatial pattern of the First Principal Component (PC1) scores (Fig. 8a) is generally consistent with the spatial patterns of summer (JJA, Fig 5a) and July (Fig. 5c) mean BSA change described previously (Sect. 3.3). PC1 scores are strongly negative (< -0.005) on western Axel Heiberg Island (large BSA declines), and weakly negative (> -0.001) or even positive at high elevations in the interiors of the*

ice masses where there was no change in the mean summer BSA. Moderately negative (~ -0.002) component scores occur on the western (continental) side of eastern Ellesmere Island's ice masses as well as over much of Manson Icefield and the southeast portion of Prince of Wales Icefield, where large decreases were observed in both the summer (JJA) and the July BSA.

For PC1, the highest Empirical Orthogonal Functions (EOFs) (32.8 and 25.9) correspond to the years with the lowest mean summer BSA (2011 and 2012) (Fig. 9). The lowest EOFs (-31.7 and -24.6) correspond to the years with the highest mean summer BSA (2013 and 2004) (Fig. 9). In addition, the departure from zero is much larger for the minimum component scores than for the maximum component scores (Fig. 8a), suggesting that both positive and negative BSA anomalies are likely caused by forcings with the same spatial pattern, albeit with the opposite sign. Investigating possible relationships between surface albedo and known large-scale patterns of atmospheric variability (Arctic Oscillation, Pacific North American Pattern, North Atlantic Oscillation), we found the EOFs for PC1 to be well (negatively) correlated with the mean summer North Atlantic Oscillation (NAO) index ($r = -0.84$, $p < 0.001$, Fig. 9), derived by averaging the June–August monthly mean NAO indices for 2001 to 2016 (http:www.cpc.ncep.noaa.gov). This is consistent with the finding of Mortimer et al. (2016) that there was a good agreement between the mean summer LST record and the NAO index in the QEI over the 2000–15 period.

The second Principal Component (PC2) had the largest EOFs of any component in 2006, 2010, and 2016. In these years, there was poor correspondence between the PC1 EOFs and the JJA NAO index (Fig. 9). The spatial pattern of the PC2 scores (Fig. 8b) resembles that of the August BSA change (Fig. 5d). Large negative PC2 scores (< -0.004) were observed on eastern Devon Ice Cap and Manson Icefield, where large August BSA declines (< -0.0075 yr^{-1}) occurred. Positive PC2 scores (Fig. 8b) were observed in southwest Axel Heiberg Island and at lower elevations on northern Ellesmere Island's southwestern ice caps, where the mean August BSA increased (Fig. 5d). Unlike PC1, there were no significant correlations between the EOFs of PC2 and known large-scale patterns of atmospheric variability.'

Revised Section 4, Lines 411-462:

'4 Discussion

Between 2001 and 2016 the bulk of the measured mean summer BSA declines in the QEI occurred in July (Sect. 3.2). This finding is consistent with previous work (e.g. Alt, 1987; Gardner and Sharp, 2007) that found variability in July near-surface air temperatures to be the primary influence on inter-annual variability in annual QEI mass balance. Variability in July air temperatures has, in turn, been associated with variations in the strength, position, and geometry of the July circumpolar vortex (Gardner and Sharp, 2007). Extreme high melt years in the QEI are associated with the intrusion of a steep ridge at all levels in the troposphere and the absence of the North American trough, making the QEI thermally homogeneous with continental North America (Alt, 1987). Between 2001 and 2016, in years with low (e.g. 2007–12) or high (e.g. 2001–04)) albedos, there was a persistent ridge (trough) in the 500 hPa geopotential height surface centered over the north and west of the QEI (Fig. 4; Sect. 3.1.1). This configuration appears to be tied to the increased warming and albedo declines observed in the central western part of the QEI from 2007 to 2012. For example, strong warming (Fig. 7b) and albedo declines (Fig. 5a) over Axel Heiberg Island and north-central Ellesmere Island coincided with a ridge of high pressure centered over the north and west of the QEI (Fig. 4) that was often observed in years when the NAO index was negative (Fig. 9).

Differences in the spatial patterns of the monthly BSA change (Fig. 5b–d) reflect the dominant atmospheric circulation patterns that occur over the QEI during the summer months. In the QEI, anticyclonic circulation tends to dominate in the months of June and July, while cyclonic circulation often occurs in August (Alt, 1987; Gascon et al., 2013). In June and July, the largest BSA declines occurred in the climatically continental interiors of the ice masses on Ellesmere and Devon Islands, as well as on Axel Heiberg Island (Fig. 5). In these months, the mountains on eastern Ellesmere and Devon Islands act as a barrier to moisture transport from the east limiting (solid) precipitation (which can temporarily raise the surface albedo) on the western (lee) side of the eastern ice masses (Koerner 1979). Adiabatic heating of descending air masses on the western (lee) side of the eastern ice masses results in warm dry air which promotes warming, melting, and enhanced albedo declines. In contrast, in August, when cyclonic circulation is common (Sect. 3.2.1), BSA declines were

largest at low elevations in the maritime regions of eastern Devon Ice Cap, Manson Icefield, and the southwestern Prince of Wales Icefield (Fig. 5d). Low pressure systems which track from the southwest to the north and northeast are common in August, and they advect warm moist air into the Arctic from the south (Alt, 1987; Gascon et al., 2013). In the eastern QEI, orographic uplift of air masses tracking from the southwest, and subsequent adiabatic heating of these air masses when they descend on the eastern sides of ice masses, would bring warm dry air to the eastern (lee) side of the mountains in the eastern QEI, promoting both warming and albedo decline in these regions in August.

During the 2001–16 period, the mean summer QEI-wide BSA record was strongly tied to the summer NAO index (Sect. 2.4). -Anticyclonic circulation was shown to co-vary with the NAO index over the Greenland Ice Sheet, immediately to the east of the QEI, since ~2001 (Rajewicz and Marshall, 2014). On the Greenland Ice Sheet, clear sky conditions and the advection of warm air form the south that accompany anticyclonic ridging (Rajewicz and Marshall, 2014), similar to that observed in the QEI in June and July (Alt, 1987; Gascon et al., 2013; Bezeau et al., 2015), were found to enhance the strength of the ice-albedo feedback between 2009 and 2011 which resulted in higher rates of melt and glacier mass loss (Box et al., 2012). Although a similar phenomenon is likely to have occurred in the QEI, we find that in some years (2006, 2010, 2016) there was poor correspondence between the mean summer BSA record and the NAO index (Fig. 9), suggesting that an additional forcing may be influencing the spatial and temporal variability of glacier surface albedo in the QEI.

The spatial pattern of both the QEI snow accumulation (Fig. 2 and 3 in Koerner 1979) and $\partial^{18}O$ values (Fig. 7 in Koerner 1979) were inferred by Koerner (1979) for the 1962-73 period from surface snow samples and shallow firn cores collected in spring 1974. These spatial patterns (of snow accumulation and $\partial^{18}O$) closely resemble the spatial pattern of PC2 scores (Fig. 8). Specifically, areas having large negative PC2 scores (< -0.002; Fig. 8b) of the 16-year mean summer BSA record (Sect. 3.4) were characterized by relatively high accumulation rates (Fig. 2 and 3 in Koerner (1979)) and snow that is isotopically warm (Fig. 7 in Koerner (1979)), while areas with positive PC2 scores had lower snow accumulation rates. This similarity points to a possible role of precipitation in affecting the mean summer BSA in some years. To investigate the relationship between the albedo record and variability in precipitation we examined the cumulative mass change record for the QEI from the Gravity Recovery and Climate Experiment (GRACE; Wolken et al. (2016), extended to 2016 (B. Wouters, personal communication, 2017)). The record shows that in 2006, 2010, and 2016 (the years when PC2 of the 16-year mean summer BSA record had the largest EOFs of any Principal Component, Sect. 3.4), once the annual minimum glacier mass was reached, there was a prolonged period of constant low mass (i.e. no melt or snowfall) before fall/winter accumulation began (inferred from an increase in mass). In other years, there was a sharp transition from the local end-of-summer mass minimum to the period of seasonally increasing mass. This could indicate that in some years during the 2001–16 period, variability in August snowfall may have influenced the mean summer BSA.'

RC: Though they point out that albedo and LST are negatively correlated for the QEI, they do not discuss that relationship as cause-and-effect in either the Abstract or the Conclusion. The relationship between albedo and LST is discussed in Section 4.2 but I would have liked that discussion to have been better integrated throughout the paper.

AR: Following a comment from an anonymous reviewer the LST analysis was revised to use MODIS C6 data instead of MODIS C5 data. The MOD11A2 C6 product has a larger amount of missing data than the C5 product. This resulted in a larger number of no-data pixels in our BSA/LST correlations (new: 46% versus old 80%) which limited our ability to confidently interpret some of the spatial patterns that were discussed in our initial submission. As such, the discussion of the relationship between albedo and temperature has been reduced compared to the original manuscript and the discussion of cause-and-effect is also reduced. However, we have tried to better integrate discussion of LST and albedo earlier in the manuscript.

Additional linkages between albedo and LST have been added earlier in the manuscript. For example, Section 3.2 has now been divided into two separate sub-sections and linkages between albedo, LST, and glacier mass change (highlighted text) have been added to Section 3.2.1. Discussion of the links between

albedo and temperature have also been added to the methods section (Sect. 2.2) where we describe the MODIS LST data and the reason for its inclusion in the manuscript, and in the results Section 3.5 (comparison of albedo and LST patterns and trends). For brevity, only a short mention of the effect that the negative ice-albedo feedback could have on the QEI ice mass is included in the Abstract. Due to the change in data set used (MOD11A2 C6) and the resulting increase in the number of cells without data, the discussion of cause and effect is reduced. Additional text regarding the relationship between temperature and albedo has been included in the conclusion.

Revised text

Section 2.2 MODIS LST (MOD11A2) added text (lines 161-168):

> *'Warmer surface temperatures increase the rates of grain metamorphism and snowmelt, resulting in larger snow grains which have a lower albedo than those of fresh snow (Wiscombe and Warren 1980; Colbeck 1982) (Sect. 1). Air and surface temperatures also affect the timing of removal of the seasonal snowpack, which exposes lower albedo firn or glacier ice. Additionally, the melt of glacier ice releases impurities that have a low albedo and thus change the surface albedo of both ice and snow (e.g. Clarke and Noone 1985; Doherty et al., 2010; Sect. 1). As such, analysis of the glacier surface temperature and comparison of these data with the albedo record is included to help understand the observed spatiotemporal patterns of glacier albedo change in the QEI.'*

Section 3.2.1 (lines 244-256), highlighted text moved from later in the manuscript and text edited for clarity:

> ***'Section 3.2.1 Mean summer (JJA) BSA anomalies***
>
> *The mean summer BSA anomalies, relative to the 2001–16 mean, are presented in Figure 3 and Table 1. For consistency with the regression analysis (Sect. 3.3), BSA anomalies were only computed for pixels having mean summer BSA observations in 11 or more of the 16 years (Sect. 2.3). The period 2001–16 is characterised by a six-year period of positive BSA anomalies (2001–06) followed by a six-year period of negative BSA anomalies (2007–12) (Table 1). Positive BSA anomalies were also observed in 2013 (+0.060) and 2014 (+0.015), while 2015 (-0.022) and 2016 (-0.005) saw a return to negative anomalies (Table 1). Negative BSA anomalies during the period 2007–12, which indicate a larger absorbed fraction of incoming shortwave radiation relative to the 16-year mean, coincide, and are consistent with, positive summer air and glacier surface temperature anomalies from 2007 to 2012 (Mortimer et al., 2016). Higher temperatures increase the rate of snow grain metamorphism which lowers the surface albedo (Wiscombe and Warren, 1980; Colbeck, 1982; Warren 1982), and a lower albedo increases the proportion of solar radiation absorbed at the ice-air interface, providing more energy for surface warming and melt. This positive feedback mechanism may have contributed to the tripling of glacier mass loss from this region between 2004–06 and 2007–09 (Gardner et al., 2011).'*

Section 3.5 Comparison with the mean summer LST, added text (lines 395-397):

> *'Owing to the positive feedback between albedo and surface temperature we would expect to observe strong increases in surface temperature where albedo declines were large. To investigate the relationship between temperature and albedo over the QEI, the 16-year mean summer LST record was compared with the 16-year mean summer BSA record (Sect. 2.3).'*

Conclusion, added text (lines 476-485):

'Albedo declines increase the proportion of incoming solar radiation absorbed at the air-ice interface, and thus the energy available to drive melt, warming, and further surface albedo decline. Warmer temperatures, in turn, increase the rate of snow grain metamorphism which lowers the albedo. Air and surface temperatures affect the removal (timing and extent) of the seasonal snowpack which exposes lower albedo firn and/or glacier ice, while melting glacier ice releases impurities that further reduce its albedo. Given that surface temperature and albedo are inextricably linked, knowing where and when albedo changes are likely to occur in future is important for predicting future rates of mass loss from the QEI ice caps. Recent investigations of atmospheric circulation patterns over the QEI (e.g. Gardner and Sharp, 2007) focused on characterization of July temperature and atmospheric conditions, since July is usually the month when melt rates peak. Our results suggest, however, that changes occurring during the month of August are also important, especially as the length of the melt season continues to increase.'

RC: The authors say that only the month of July shows statistically-significant albedo decrease over the study period. Thus, they should consider stating that the July albedo is decreasing over the study period instead of saying mean summer (JJA) albedo is decreasing.

AR: There appears to have been some misinterpretation of our results. No measurable changes in the June or August QEI-wide (regionally-averaged) BSA were observed owing to the large amount of spatial variability in the sign and magnitude of BSA change in these months. Measurable changes were observed in the mean summer (JJA) and mean July QEI-wide BSA. These changes, however, were not statistically significant at the $p < 0.05$ level. Although there were statistically significant (at the $p < 0.05$ confidence level) decreases in the mean summer (JJA) and/or July BSA at the pixel scale, this was not the case for either the mean summer (JJA) or July QEI-wide (spatially averaged) BSA change. As such, our conclusions and abstract remain unchanged. Text in the results section 3.3.1 (lines 306-308) has been revised for clarity.

Revised text:

> **Results section 3.3.1 lines 318-320*: 'Although the measured change in the QEI-wide mean summer BSA (average correlation coefficient of all pixels) was not statistically significant ($r = 0.31$, $p = 0.24$), BSA declines that were significant at the $p \leq 0.05$ level were observed at the pixel scale on all ice masses (Fig. 6a).'***

Reviewer 1 specific comments:

RC 1 Title: consider removing "C6" from the title since it's not that different from C5 for the albedo and LST, and many people, before reading the paper, have no idea what C6 is. You have appropriately mentioned the fact that you've used C6 in the paper as needed. Also consider including LST in the title, especially if you decide to enhance the discussion about cause-and-effect between LST and albedo for the QEI.

AR 1: Reference to "C6" removed from the title. The title has also been modified to better reflect the content of the paper. Instead of 'Characterization of' we use 'Spatiotemporal variability of' to indicate that the paper investigates both the spatial and temporal patterns of glacier surface albedo in the Canadian High Arctic.

Revised title:

> '*Spatiotemporal variability of Canadian High Arctic glacier surface albedo from MODIS data, 2001-16'*

RC 2: Figure 1 caption: do you mean "Top-left inset" and "Bottom-right inset"?

AR 2: Bottom-left inset in Figure 1 removed and caption corrected.

Revised Figure 1 caption:

'*Figure 1: Glaciated regions of the Queen Elizabeth Islands. Background image: MODIS, 4 July 2011. Inset: red polygon shows location of Queen Elizabeth Islands, Arctic Canada.'*

RC 3: Figures 2,3,5,6,7&9: it should be mentioned in the caption that white (Figs 2 & 3) is not ice and brown is not ice (Figs 5,6,7, & 9).

AR 3: Mention of white areas (Fig. 2 & 3) and brown (Fig. 5, 6, 7, 9 (now Figure 8)) areas that are not ice has been added to the figure captions.

Revised Figure captions:

'Figure 2: Mean summer clear-sky shortwave broadband black-sky albedo over the QEI ice caps. White areas outside of the ice caps indicate non-glaciated ice cover.

Figure 3: Mean summer clear-sky shortwave broadband albedo anomaly over the QEI ice caps relative to the 2001-16 mean. White areas outside of the ice caps indicate non-glaciated ice cover.

Figure 5: Linear rate of change (yr^{-1}) in (a) mean summer (JJA), (b) June, (c) July, and (b) August, clear-sky shortwave broadband black-sky albedo for 2001-16 over the QEI ice caps. Background image: MODIS, 4 July 2011. Brown indicates non-glaciated land cover.

Figure 6: p-value of the linear regression (Fig. 4) of (a) mean summer (JJA), (b) June, (c) July, and (d) August, clear-sky shortwave broadband black-sky albedo for the period 2001-16 over the QEI ice caps. Background image: MODIS, 4 July 2011. Brown indicates non-glaciated land cover.

Figure 7: Component scores for the first two Principal Components of the mean summer clear-sky BSA (Fig. 2) over the QEI ice caps. Background image: MODIS, 4 July 2011. Brown indicates non-glaciated land cover.

Figure 8: (a) Pearson Correlation Coefficient (r) and (b) p-value for linear regression of the 16 year BSA and LST record over the QEI ice caps. Background image: MODIS, 4 July 2011. Brown indicates non-glaciated land cover.'

RC 4: Figure 8 – lower panel: I am confused about the point that you are trying to get across in this graph; please clarify.

AR 4: The lower panel of Figure 8 (which is now Figure 9) illustrates the correspondence between the Empirical Orthogonal Functions for the first and second Principal Components of the 16 year mean summer BSA record, respectively, and the mean summer NAO index. The graph presents the EOFs of PC1 and PC2 of both the mean summer (JJA) BSA record and the mean summer (JJA) NAO index for each year during the period 2001-16.

The original legend on the lower panel of Figure 8 (now Figure 9) did not include the NAO index. This may have been a source of confusion. The legend has been modified to include the NAO index (black line) and a reference to Section 3.4 where this graph is discussed, has been added.

Modified Figure 9 with figure caption:

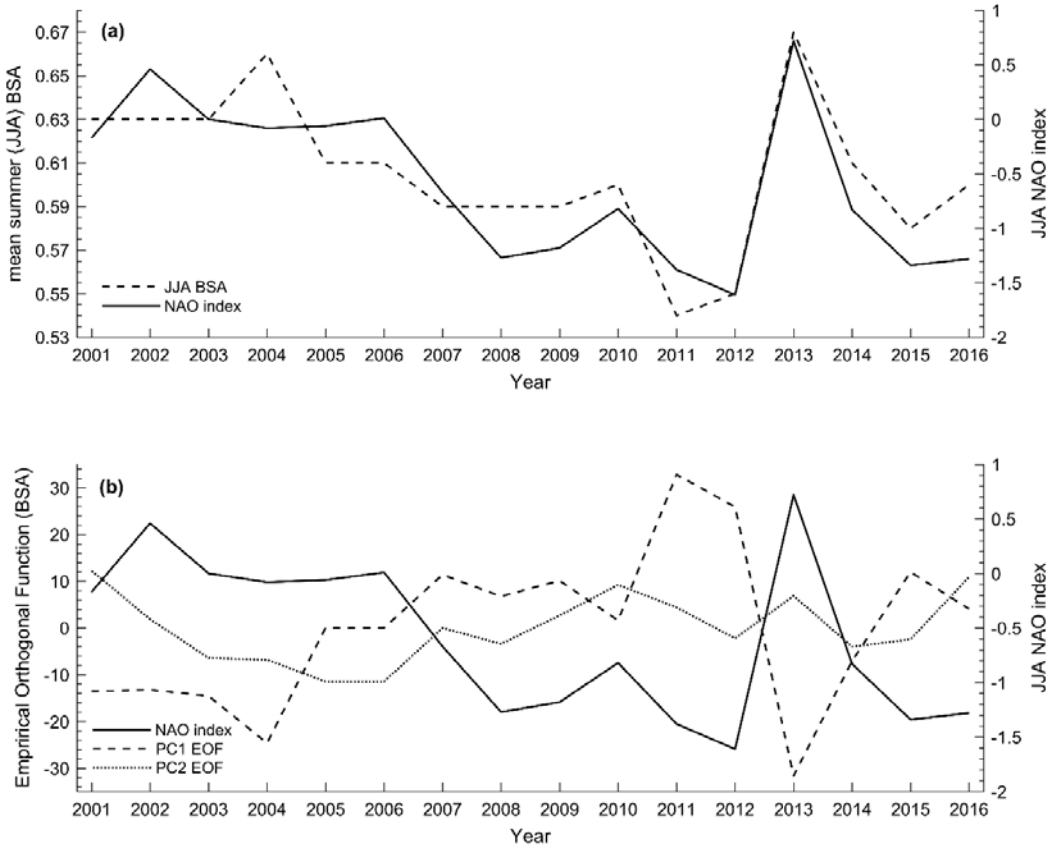

'Figure 9: (a) mean summer (JJA) clear-sky shortwave broadband black-sky albedo (left-hand axis) and the mean summer (JJA) NAO index (right-hand axis) for 2001-16. (b) Empirical Orthogonal Functions (EOF) for the First and Second Principal Components of the 16 year mean summer BSA record (left-hand axis), and the mean summer (JJA) NAO index (right-hand axis) for 2011-2016 (Sect. 3.4). '

RC 5: Line 14: note that the range of years says 2008-2012 on line 486

AR 5: Corrected to read 2007-12 throughout.

Revised text:

Line 12-14: *'Most of the decrease in BSA, which was greatest at lower elevations around the margins of the ice masses, occurred between 2007 and 2012 when mean summer BSA was anomalously low.'*

Line247-248: *'The period 2001–16 is characterised by a six-year period of positive BSA anomalies (2001–06) followed by a six-year period of negative BSA anomalies (2007–12) (Table 1).'*

Line 250-252: *'Negative BSA anomalies during the period 2007–12, which indicate a larger absorbed fraction of incoming shortwave radiation relative to the 16-year mean, coincide, and are consistent with, positive summer air and glacier surface temperature anomalies from 2007 to 2012 (Mortimer et al., 2016).'*

Line 278-279: *'… in years when the mean summer QEI-wide BSA anomaly was strongly negative (e.g. 2001–04) (or positive (e.g. 2007–12))'*

Line 418-420: *'Between 2001 and 2016, in years with low (e.g. 2007–12) or high (e.g. 2001–04)) albedos, there was a persistent ridge (trough) in the 500 hPa geopotential height surface centered over the north and west of the QEI (Fig. 4; Sect. 3.1.1).'*

Line 466-467: *'Strong negative BSA anomalies from 2007–12 suggest that the bulk of the observed albedo decline occurred during this six-year period.'*

RC 6 Line 60: MODIS has already been defined on lines 53 & 54

AR 6: Corrected.

Revised line 60 (now line 61):

'Observations from the MODIS sensors, aboard the Terra (2000 to present) and Aqua (2002 to present) satellites,…'

RC 7 Line 76 & 78: Lutch should be spelled Lucht

AR 7: Misspelled reference corrected in **lines 76 & 78 (now lines 77 & 79)**

Revised text:

Line 77: *'…kernel-driven BRDF model (Wanner et al., 1997; Lucht et al., 2000; Schaaf et al., 2002, 201b).'*

Line 79: '*…is used to estimate the surface albedo (Strugnell and Lucht, 2001; Schaaf et al., 2002; Jin et al., 2003; Liu et al., 2009).'*

RC 8 Line 99: perhaps the word "detectors" should be used instead of "instruments"?

AR 8: The word "instruments" replaced by "detectors".

Revised **Line 99 (now line 91-92:**

'*The MODIS sensors are currently operating well beyond their expected [productive] six year lifetimes (Barnes et al, 1998; Justice 1998) and the detectors are degrading (Xiong et al., 2001).'*

RC 9 Line 120-124: this discussion of MOD10A1 should be deleted; it is not relevant to this paper, and MOD10A1 is never mentioned again in the paper; it really isn't good validation for MCD43A3.

AR 9: Discussion of MOD10A1 has been deleted. Additionally, in response to an anonymous reviewer's comments, this section has been revised to be more informative regarding MODIS sensor design and capabilities.

Revised text, lines 90-138:

'2.1.1 MODIS sensor degradation

The MODIS sensors are currently operating well beyond their expected [productive] six year lifetimes (Barnes et al, 1998; Justice 1998) and the detectors are degrading (Xiong et al., 2001). For both the MODIS Terra and Aqua sensors, instruments were calibrated pre-launch (radiometric, spatial, specular calibration) (Gunther et al., 1996). On-orbit calibration procedures were included to monitor the sensor degradation that is expected as the instruments are exposed to solar radiation (Gunther et al., 1996). For the reflective solar bands (0.41–2.2 μm) the on-board calibration system includes a solar diffuser (SD) calibrated using the solar diffuser stability monitor (SDSM) (Gunther et al., 1998). Lunar and Earth view observations (for select desert sites) are also used to assess radiometric stability (Sun et al., 2003). Even so, long-term scan mirror and wavelength dependent degradation, which are not sufficiently accounted for by the on-board calibrators (SD/SDMS), have been observed (Xiong et al., 2001; Lyapustin et al., 2014 and references therein). Calibration degradation effects, which are largely confined to the MODIS Terra sensor, are greatest in the

blue band (B3) and decrease with increasing wavelength (Xiong and Barnes, 2006). An anomaly in the SD door operation (3 May 2003) and a decision to leave the door permanently open, exposing the SD to additional solar radiation, resulted in degradation of the SD on the MODIS Terra sensor that was faster than had originally been anticipated, and than was observed for the MODIS Aqua sensor (Xiong et al., 2005). Differences in the response versus scan angle (RVS) for the two side mirrors were also characterized pre-launch (Barnes et al., 1998). The RVS is important because it describes the scan mirror's response to different angles of incidence (AOI, for each band, detector and mirror side) (Sun et al., 2014). However, for the MODIS Terra sensor, following an overheating incident during pre-launch calibration, the RVS was not re-characterized and the exact pre-launch RVS characteristics are not known (Pan et al., 2007; Sun et al., 2014 and references therein). These issues have resulted in the performance of the MODIS Terra sensor being poorer than that of the MODIS Aqua sensor.

As a normal part of the operational procedure, the MODIS Characterization Support Team (http:mcst.gsfc.nasa.gov) periodically updates the calibration algorithms and approaches, during which time the entire L1B record (calibrated top of the atmosphere radiances) is re-processed to reflect improved understanding and characterization of changes to the instruments. Even so, non-physical trends in MODIS Terra data products, that result from calibration drift, have been observed and are well documented (e.g. Xiong et al., 2001; Xiong and Barnes, 2006; Franz et al., 2008; Kwiatkowski et al., 2008; Wang et al., 2012; Lyapustin et al., 2014; and references therein). The latest revision occurred with the C6 data and includes on-orbit calibration procedures to mitigate long-term calibration drift, particularly at the shorter wavelengths (Wenny et al., 2010; Toller et al., 2013; Sun et al., 2014; Lyapustin et al., 2014). The C6 dataset uses the on-board calibrators (e.g. SD/SDMS) and the mirror side ratios from lunar standard and Earth view observations (Toller et al, 2013; Sun et al., 2014). The C6 revision also includes an additional approach, aimed primarily at the short-wavelength bands, that uses observations of desert sites (pseudo-invariant targets) to derive instrument calibration coefficients and RVS at multiple AOIs (instead of the two AOIs provided by the SD and lunar standard) (Toller et al, 2013; Sun et al., 2014). Although this vicarious approach is less accurate than the one that uses the mirror-side ratios calibrated using a lunar standard, it has been found to provide a significant improvement to the L1B radiance measurements relative to the C5 data, prior to ~2013 (Toller 2013; Lyapustin et al., 2014). Updated L1B C6 radiances can be up to several percent higher than the C5 values (e.g. Band 3 and for most recent period ~2013 onward) (Toller et al., 2013; Lyapustin et al. 2014; Casey et al., 2017). However, evaluation of the L1B C6 Band 3 (0.46–0.48 µm) radiance over a desert site (Libya 4) identified residual errors (decadal trends on the order of several tenths of 1%; Lyapustin et al., 2014) that are within the product's stated accuracy (2% in absolute reflectance units for the reflective solar bands (Barnes et al., 1998; Justice et al., 1998)). The impact of the C6 updates on higher level MODIS science products is difficult to quantify because the corrections are time, mirror-side, angular, and detector dependent (Toller et al., 2013; Lyapustin et al. 2014; Sun et al., 2014). In addition, the C6 revision includes updates to algorithms (in addition to the calibration updates) used in the derivation of specific higher-level products (https://www.umb.edu/spectralmass/terra_aqua_modis/v006 outlines changes made to the MCD43A3 C6 data product). Important for the current study, however, is that recent analysis of surface albedo over the Greenland Ice Sheet, immediately to the east of the QEI, using MODIS C6 data (including the MCD43A3 product used in this study) identified statistically significant albedo declines over the wet snow zone (Casey et al., 2017). For the most part, these declines are thought to be physically real (Casey et al., 2017), which gives us confidence in the albedo trends presented here. There are no long-term, spatially distributed, in situ albedo records from the glaciers and ice caps in the QEI, so a comparison between the MCD43A3 records and ground observations is not possible. This is both a motivation for and a limitation of, the current study.

References added:

Barnes, W. L., Pagano, T.S., and Salomonson V.V.: Prelaunch characteristics of the Moderate Resolution Imaging Spectroradiometer (MODIS) on EOS-AM1, IEEE Transactions on Geoscience and Remote Sensing, 36(4), 1088-1100, doi: 10.1109/36.700993, 1998.

Franz, B.A., Kwiatkowska, E.J., Meister, G. and McClain, C.R.: Moderate Resolution Imaging Spectroradiometer on Terra: limitations for ocean color applications, Journal of Applied Remote Sensing, 2(1), 023525, doi: 10.1117/1.2957964, 2008.

Guenther, B., Barnes, W., Knight, E., Barker, J., Harnden, J., Weber, R., Roberto, M., Godden, G., Montgomery, H., and Abel, P.: MODIS calibration: a brief review of the strategy for the at-launch calibration approach, Journal of Atmospheric and Oceanic Technology, 13(2), 274-285. doi: 10.1175/1520-0426(1996)013<0274:MCABRO>2.0.CO;2, 1996

Guenther, B. Godden, G. D., Xiong, X., Knight, E.J., Qiu, S. Y., Montgomery, H., Hopkins, M. M., Khayat, M. G., and Zhidong Hao, Z.: Prelaunch algorithm and data format for the Level 1 calibration products for the EOS-AM1 Moderate Resolution Imaging Spectroradiometer (MODIS), IEEE Transactions on Geoscience and Remote Sensing, 36(4), 1142-1151, doi: 10.1109/36.701021, 1998.

Justice, C.O., Vermote, E., Townshend, J.R.G., Defries, R., Roy, D. P., Hall, D. K., Vincent V. Salomonson V. V. et al.: The Moderate Resolution Imaging Spectroradiometer (MODIS): Land remote sensing for global change research, IEEE Transactions on Geoscience and Remote Sensing, 36(4), 1228-1249, doi: 10.1109/36.701075, 1998.

Kwiatkowska, E. J., Franz, B. A., Meister, G., McClain, C. R., and Xiong, X.: Cross calibration of ocean-color bands from Moderate-Resolution Imaging Spectroradiometer on Terra platform, Applied Optics, 47(36), 6796–6810, doi:10.1364/AO.47.006796, 2008.

Pan C., Xiong, X., Che, N.: MODIS pre-launch characterization of reflective solar bands response vs. Scan angle, Proc. SPIE – Earth Observeing Systems XII, Optical Engineering Applications, 66770R, doi:10.117/12.730573, 2007.

Sun, J., Xiong, X., Guenther, B., and Barnes, W.: Radiometric stability monitoring of the MODIS reflective solar bands using the Moon, Metrologia, 40(1), S85, doi: 10.1088/0026-1394/40/1/319, 2003.

Sun, J., Xiong, X., Angal, A., Chen, H., Wu, A., and Geng, X.: Time-dependent response versus scan angle for MODIS reflective solar bands, IEEE Transactions on Geoscience and Remote Sensing, 52(6), 3159-3174, doi: 10.1109/TGRS.2013.2271448, 2014.

Wenny, B. N., Sun, J., Xiong, X., Wu, A., Chen, H., Angal, A., Choi, T., Madhavan, S., Geng, X., Kuyper, J., and Tan, L.: MODIS calibration algorithm improvements developed for Collection 6 Level-1B, Proc. SPIE – Earth Observing Systems XV, 78071F, doi: 10.1117/12.860892, 2010.

Xiong, X., Esposito, J., Sun, J., Pan, C., Guenther, B., and Barnes, W. L.: Degradation of MODIS optics and its reflective solar bands calibration, In Proc. SPIE – Sensors, Systems, and Next-Generation Satellites V, 4540, 62-70. Doi: 10.1117/12.450646, 2001.

Xiong, X., Eriyes, H., Xiong, S., Xie, X., Esposito, J., Sun, J., and Barnes, W.: Performance of Terra MODIS solar diffuser and solar diffuser stability monitor, In Proc. SPIE - Earth Observing Systems X, 58820S doi: 10.1117/12.615334, 2005.

Xiong, X., and Barnes, W.: An overview of MODIS radiometric calibration and characterization, Advances in Atmospheric Sciences, 23(1), 69-79, doi: 10.1007/s00376-006-0008-3, 2006.

RC 10 Line 151: This is misleading because, in Hall et al (2008a), the pixels when the temperature was >2 deg C were removed since it's impossible to have a temperature greater than zero and still be ice. Hall et al. (2008a) did not remove pixels with errors >2 deg C that were below zero, if I am recalling correctly.

RC 10.1: Hall et al. (2008a) did not remove pixels with errors >2 deg C that were below zero, if I am recalling correctly.

AR 10.1: You are correct in pointing out that Hall et al. 2008a did not remove pixels with errors >2°C that were below 0°C. Hall et al. (2008a) developed melt-frequency maps and identified any pixels with a LST >0°C as experiencing melt. The inclusion of Hall et al. (2008a) at the end of this sentence is, as you say, incorrect and misleading. As such, the reference to Hall et al. (2008a) has been removed and only the reference to Mortimer et al. (2016) is included.

Revised text, Line 151 (now line 177-179):

'Pixels for which the average LST error (QC_Day LST error flag) exceeded 2°C were removed from the analysis and any remaining pixels having a temperature >0°C were assigned a temperature of 0°C (Mortimer et al., 2016).'

RC 10.2: …'it's impossible to have a temperature greater than zero and still be ice.':

AR 10.2: Although the temperature of pure ice and snow cannot exceed 0°C, many pixels are not comprised solely of pure ice and snow. Rock, dust, impurities and ponded water (for which the maximum temperature can exceed 0°C) can exist on the snow/ice surface. The presence of these materials within the 1km x 1km pixel can result in an LST >0°C. Mortimer et al. (2016) found that pixels having an LST >0°C were mainly located on outlet glaciers and near the ice-cap margins and inferred that such pixels probably contained a mixture of exposed rock, ice, and meltwater during the melt season. The presence of materials other than pure ice and snow within a pixel can, therefore, result in an LST greater than the maximum temperature of pure ice and snow. To mitigate this effect, ice-covered pixels with an LST >0°C were reassigned a value of 0°C.

RC 11 Line 155: it should be stated that MOD11A2 Collection 6 data were downloaded

AR 11 Corrected

Revised Line 155 (now line 183-185):

'MOD11A2 C6 data were downloaded from (https://lpdaac.usgs.gov/, accessed September–October 2017) and re-projected to a North America Albers Equal Area projection, WGS84 datum, 1 km resolution.'

RC 12 Line 235: I would say "opposite from" instead of "opposite to"

AR 12 This text, as written, is not included in the revised manuscript.

RC 13 Line 319: I think sections 3.3 and 4.1 could be shortened and made to be more concise.

AR 13 Sections 3.3 (now section 3.4) and 4.1 (now section 4) have been shortened. Repetition in sections 3.3 and 4.1 has been removed. Sections 4.1 and 4.2 have been merged (now section 4).

Revised Section 3.4, Lines 365-392:

'3.4 Principal Components Analysis

To explore whether there are any other spatial patterns in the 16-year mean summer BSA record that differ from the long-term (linear) trend, we performed a Principal Components Analysis of the BSA record (Sect. 2.3). The first and second Principal Components (Fig. 8) explain 65% and 12% of the variance in the mean summer BSA record, respectively. The spatial pattern of the First Principal Component (PC1) scores (Fig. 8a) is generally consistent with the spatial patterns of summer (JJA, Fig 5a) and July (Fig. 5c) mean BSA change described previously (Sect. 3.3). PC1 scores are strongly negative (< -0.005) on western Axel Heiberg Island (large BSA declines), and weakly negative (> -0.001) or even positive at high elevations in the interiors of the ice masses where there was no change in the mean summer BSA. Moderately negative (~ -0.002) component scores occur on the western (continental) side of eastern Ellesmere Island's ice masses as well as over much of Manson Icefield and the southeast portion of Prince of Wales Icefield, where large decreases were observed in both the summer (JJA) and the July BSA.

For PC1, the highest Empirical Orthogonal Functions (EOFs) (32.8 and 25.9) correspond to the years with the lowest mean summer BSA (2011 and 2012) (Fig. 9). The lowest EOFs (-31.7 and -24.6) correspond to the years with the highest mean summer BSA (2013 and 2004) (Fig. 9). In addition, the departure from zero is much larger for the minimum component scores than for the maximum component scores (Fig. 8a), suggesting that both positive and negative BSA anomalies are likely caused by forcings with the same spatial

pattern, albeit with the opposite sign. Investigating possible relationships between surface albedo and known large-scale patterns of atmospheric variability (Arctic Oscillation, Pacific North American Pattern, North Atlantic Oscillation), we found the EOFs for PC1 to be well (negatively) correlated with the mean summer North Atlantic Oscillation (NAO) index ($r = -0.84$, $p < 0.001$, Fig. 9), derived by averaging the June–August monthly mean NAO indices for 2001 to 2016 (http:www.cpc.ncep.noaa.gov). This is consistent with the finding of Mortimer et al. (2016) that there was a good agreement between the mean summer LST record and the NAO index in the QEI over the 2000–15 period.

The second Principal Component (PC2) had the largest EOFs of any component in 2006, 2010, and 2016. In these years, there was poor correspondence between the PC1 EOFs and the JJA NAO index (Fig. 9). The spatial pattern of the PC2 scores (Fig. 8b) resembles that of the August BSA change (Fig. 5d). Large negative PC2 scores (< -0.004) were observed on eastern Devon Ice Cap and Manson Icefield, where large August BSA declines (< -0.0075 yr^{-1}) occurred. Positive PC2 scores (Fig. 8b) were observed in southwest Axel Heiberg Island and at lower elevations on northern Ellesmere Island's southwestern ice caps, where the mean August BSA increased (Fig. 5d). Unlike PC1, there were no significant correlations between the EOFs of PC2 and known large-scale patterns of atmospheric variability.'

Revised Section 4, Lines 411-462:

'4 Discussion

Between 2001 and 2016 the bulk of the measured mean summer BSA declines in the QEI occurred in July (Sect. 3.2). This finding is consistent with previous work (e.g. Alt, 1987; Gardner and Sharp, 2007) that found variability in July near-surface air temperatures to be the primary influence on inter-annual variability in annual QEI mass balance. Variability in July air temperatures has, in turn, been associated with variations in the strength, position, and geometry of the July circumpolar vortex (Gardner and Sharp, 2007). Extreme high melt years in the QEI are associated with the intrusion of a steep ridge at all levels in the troposphere and the absence of the North American trough, making the QEI thermally homogeneous with continental North America (Alt, 1987). Between 2001 and 2016, in years with low (e.g. 2007–12) or high (e.g. 2001–04)) albedos, there was a persistent ridge (trough) in the 500 hPa geopotential height surface centered over the north and west of the QEI (Fig. 4; Sect. 3.1.1). This configuration appears to be tied to the increased warming and albedo declines observed in the central western part of the QEI from 2007 to 2012. For example, strong warming (Fig. 7b) and albedo declines (Fig. 5a) over Axel Heiberg Island and north-central Ellesmere Island coincided with a ridge of high pressure centered over the north and west of the QEI (Fig. 4) that was often observed in years when the NAO index was negative (Fig. 9).

Differences in the spatial patterns of the monthly BSA change (Fig. 5b–d) reflect the dominant atmospheric circulation patterns that occur over the QEI during the summer months. In the QEI, anticyclonic circulation tends to dominate in the months of June and July, while cyclonic circulation often occurs in August (Alt, 1987; Gascon et al., 2013). In June and July, the largest BSA declines occurred in the climatically continental interiors of the ice masses on Ellesmere and Devon Islands, as well as on Axel Heiberg Island (Fig. 5). In these months, the mountains on eastern Ellesmere and Devon Islands act as a barrier to moisture transport from the east limiting (solid) precipitation (which can temporarily raise the surface albedo) on the western (lee) side of the eastern ice masses (Koerner 1979). Adiabatic heating of descending air masses on the western (lee) side of the eastern ice masses results in warm dry air which promotes warming, melting, and enhanced albedo declines. In contrast, in August, when cyclonic circulation is common (Sect. 3.2.1), BSA declines were largest at low elevations in the maritime regions of eastern Devon Ice Cap, Manson Icefield, and the southwestern Prince of Wales Icefield (Fig. 5d). Low pressure systems which track from the southwest to the north and northeast are common in August, and they advect warm moist air into the Arctic from the south (Alt, 1987; Gascon et al., 2013). In the eastern QEI, orographic uplift of air masses tracking from the southwest, and subsequent adiabatic heating of these air masses when they descend on the eastern sides of ice masses, would bring warm dry air to the eastern (lee) side of the mountains in the eastern QEI, promoting both warming and albedo decline in these regions in August.

During the 2001–16 period, the mean summer QEI-wide BSA record was strongly tied to the summer NAO index (Sect. 2.4). -Anticyclonic circulation was shown to co-vary with the NAO index over the Greenland Ice

Sheet, immediately to the east of the QEI, since ~2001 (Rajewicz and Marshall, 2014). On the Greenland Ice Sheet, clear sky conditions and the advection of warm air form the south that accompany anticyclonic ridging (Rajewicz and Marshall, 2014), similar to that observed in the QEI in June and July (Alt, 1987; Gascon et al., 2013; Bezeau et al., 2015), were found to enhance the strength of the ice-albedo feedback between 2009 and 2011 which resulted in higher rates of melt and glacier mass loss (Box et al., 2012). Although a similar phenomenon is likely to have occurred in the QEI, we find that in some years (2006, 2010, 2016) there was poor correspondence between the mean summer BSA record and the NAO index (Fig. 9), suggesting that an additional forcing may be influencing the spatial and temporal variability of glacier surface albedo in the QEI.

The spatial pattern of both the QEI snow accumulation (Fig. 2 and 3 in Koerner 1979) and $\partial^{18}O$ values (Fig. 7 in Koerner 1979) were inferred by Koerner (1979) for the 1962-73 period from surface snow samples and shallow firn cores collected in spring 1974. These spatial patterns (of snow accumulation and $\partial^{18}O$) closely resemble the spatial pattern of PC2 scores (Fig. 8). Specifically, areas having large negative PC2 scores (< -0.002; Fig. 8b) of the 16-year mean summer BSA record (Sect. 3.4) were characterized by relatively high accumulation rates (Fig. 2 and 3 in Koerner (1979)) and snow that is isotopically warm (Fig. 7 in Koerner (1979)), while areas with positive PC2 scores had lower snow accumulation rates. This similarity points to a possible role of precipitation in affecting the mean summer BSA in some years. To investigate the relationship between the albedo record and variability in precipitation we examined the cumulative mass change record for the QEI from the Gravity Recovery and Climate Experiment (GRACE; Wolken et al. (2016), extended to 2016 (B. Wouters, personal communication, 2017)). The record shows that in 2006, 2010, and 2016 (the years when PC2 of the 16-year mean summer BSA record had the largest EOFs of any Principal Component, Sect. 3.4), once the annual minimum glacier mass was reached, there was a prolonged period of constant low mass (i.e. no melt or snowfall) before fall/winter accumulation began (inferred from an increase in mass). In other years, there was a sharp transition from the local end-of-summer mass minimum to the period of seasonally increasing mass. This could indicate that in some years during the 2001–16 period, variability in August snowfall may have influenced the mean summer BSA.'

RC 14 Line 601: should read IEEE instead of IEE

AR 14 Reference corrected (IEEE instead of IEE)

Revised text:

'Salomon, J. G., Schaaf, C. B., Strahler, A. H., Gao, F., and Jin, Y.: Validation of the MODIS Bidirectional Reflectance Distribution Function and Albedo retrievals using combined observations from the Aqua and Terra platforms, IEEE Transactions on Geoscience and Remote Sensing, 44(6), 1555-1565, 2006.'